

# Theory of Scanning Tunneling Spectroscopy of Magnetic-Field-Induced Discrete Nodal States in a $d$ -Wave Superconductor

Boldizsár Jankó

Materials Science Division, Argonne National Laboratory, 9700 South Cass Avenue, Argonne, Illinois 60439  
(Received 23 December 1998)

In the presence of an external magnetic field, the low lying elementary excitations of a  $d$ -wave superconductor have quantized energy and their momenta are locked near the node direction. It is argued that these discrete states can most likely be detected by a local probe, such as a scanning tunneling microscope. The low temperature *local* tunneling conductance on the Wigner-Seitz cell boundaries of the vortex lattice is predicted to show peaks spaced as  $\pm\sqrt{n}$ ,  $n = \{0, 1, 2, \dots\}$ . Away from the cell boundary, where the superfluid velocity is nonzero, each peak splits, in general, into four peaks, corresponding to the number of nodes in the order parameter. [S0031-9007(99)09303-5]

PACS numbers: 74.25.Jb, 61.16.Ch, 74.60.Ec, 74.72.Hs

The nature of the quasiparticle spectrum in the Abrikosov vortex state of the cuprate superconductors has attracted strong continuing interest in recent years [1]. There are two main reasons why this spectrum is expected to be unconventional. First, the pair size  $\xi_0$  seems to be comparable to the interparticle distance  $1/k_F$ . Indeed, angle-resolved photoemission experiments [2] on  $\text{Bi}_2\text{Sr}_2\text{CaCu}_2\text{O}_{8+x}$  give  $k_F \sim 0.7 \text{ \AA}^{-1}$ , while magnetization studies [3] indicate that  $\xi_0 \sim 10\text{--}15 \text{ \AA}$ . Second, there is by now substantial experimental evidence [4] for nodes in the cuprate superconducting gap. In contrast to conventional superconductors, where the main source of low lying excitations in the mixed state are the bound vortex core states [5], the above mentioned reasons turn the bound core states into a delicate feature [6–8] of cuprate superconductors. Experiments seem to mirror this uncertainty: while bound core states were observed in  $\text{YBa}_2\text{Cu}_3\text{O}_{6-\delta}$  by far-infrared spectroscopy [9] and scanning tunneling spectroscopy (STS) [10], their presence in  $\text{Bi}_2\text{Sr}_2\text{CaCu}_2\text{O}_{8+x}$  is controversial [11].

The aim of the present paper is to point out that a discrete spectrum should nevertheless be observable in the *local* density of states of the mixed state of all cuprates. It is somewhat unexpected, however, that such a spectrum is more likely to be observable close to the Wigner-Seitz cell boundaries of the Abrikosov lattice, where the superfluid velocity is small. This is in contrast to conventional Caroli–de Gennes–Matricon bound states [5], which appear in the vortex core, in the region of singular superflow. STS is an ideal probe [12] to detect these low lying discrete states, provided that the intervortex region is studied, and not the core region, where the recent STS studies [10,11] were focused so far. The existence of field-induced discrete quasiparticle states in a superfluid with gap nodes was suggested by Volovik [13] for the  $A$  phase of superfluid  $^3\text{He}$ , where an effective magnetic field is supplied by a static order parameter texture. The analog of these nodal states in cuprate superconductors was recently proposed by Gor'kov and Schrieffer [14], as the appropriate basis states for discussing the de Haas–van Alphen oscillations in the

mixed state of a  $d$ -wave superconductor. Quite recently, Anderson [15] attributed the anomalous magnetothermal conductivity of  $\text{Bi}_2\text{Sr}_2\text{CaCu}_2\text{O}_{8+x}$  [16] to the appearance of the magnetic-field-induced discrete spectrum at the gap nodes. These global probes, however, cannot provide direct spectroscopic evidence for such a fine structure in the electron spectrum: spatial averaging results in averaging over large Doppler shifts [17] due to the supercurrents surrounding the vortices, which in turn act to smear out the discrete level spectrum [18]. One can anticipate the existence of such a discrete spectrum by the following quasi-classical argument. Let us take a two-dimensional circular Fermi surface for the quasiparticles in the  $(a, b)$  plane and orient the magnetic field  $\mathbf{B}$  along the  $c$  axis [see Fig. 1(a)]. The quasiparticle equation of motion in the normal state is

$$\partial_t \mathbf{k} = \frac{e}{c\hbar} \mathbf{v}_\mathbf{k} \times \mathbf{B} - \frac{\mathbf{k}}{\tau}, \quad (1)$$

where  $\mathbf{v}_\mathbf{k} = \hbar^{-1} \partial_\mathbf{k} \epsilon(\mathbf{k})$  is the quasiparticle velocity. While the normal state quasiparticles are strongly damped, the quasiparticle lifetime  $\tau$  increases rapidly below the superconducting transition [19]. If that would be the only change for temperatures below  $T_c$ , the solution to the above equation could be given in terms of a phase

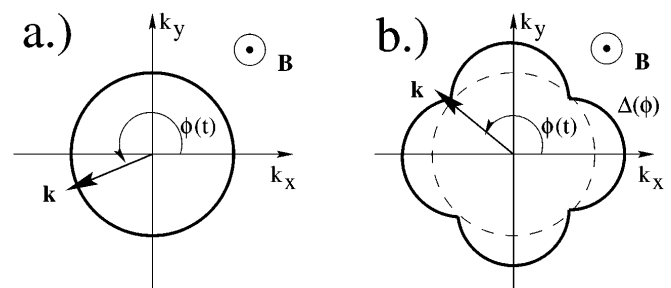


FIG. 1. (a) Schematic picture of a normal state quasiparticle momentum precessing according to  $\phi(t) = \omega_c t$ ; (b) in the presence of an anisotropic order parameter, the quasiparticle momenta of the low-lying excitations are bound to the node region  $\phi_j = (2j + 1)\pi/4$ ,  $j = \{0, 1, 2, 3\}$ .

variable  $\mathbf{k} = k(\cos\phi(t), \sin\phi(t))$ ,

$$\phi(t) = \omega_c \frac{c\hbar}{eB} \int_{FS} \frac{dk}{v_k} = \omega_c t, \quad (2)$$

where  $\omega_c = eB/m^*c$ . More importantly, however, the onset of superconductivity generates the appearance of a gap tied to the entire Fermi circle [see Fig. 1(b)]. If  $\Delta(\phi)$  is anisotropic, such as in the case of a  $d$ -wave superconductor with  $\Delta(\phi) = \Delta_0 \cos(2\phi)$ , the order parameter will provide an off-diagonal confining potential in the angular coordinate space, for the Bogoliubov quasiparticles precessing around the Fermi surface.

In order to provide a more detailed discussion of these phenomena, it is necessary to obtain the quasiparticle amplitudes  $u_n(\phi), v_n(\phi)$ . Let us focus on the intermediate field regime  $B_{c1} \ll B \ll B_{c2}$  when the field in the sample is fairly uniform, and address the effect of superflow later. It is most convenient to use the Bogoliubov-de Gennes equations for the angular amplitudes of quasiparticles near the Fermi surface  $k \sim k_F$ , in the form given by Gor'kov and Schrieffer [14,20],

$$(E_n - i\hbar\omega_c\partial_\phi + \bar{\mu})u_n(\phi) + \Delta(\phi)v_n(\phi) = 0, \quad (3)$$

$$(E_n + i\hbar\omega_c\partial_\phi - \bar{\mu})v_n(\phi) + \Delta(\phi)u_n(\phi) = 0,$$

where  $\bar{\mu}$  is defined by  $\mu - \bar{\mu} = \omega_c N_0$  ( $N_0$  is a large integer). In this approximation, the dependence of the gap and the amplitudes on the radial component of the momentum is neglected, and the angle  $\phi$  remains the only dynamic variable. The amplitudes obey periodic boundary conditions  $(u_n(\phi), v_n(\phi)) = (u_n(\phi + 2\pi), v_n(\phi + 2\pi))$ . The normalization conditions are

$$\int_{-\pi}^{\pi} \frac{d\phi}{2\pi} [|u_n(\phi)|^2 + |v_n(\phi)|^2] = 1. \quad (4)$$

which can be recognized as the Schrödinger equation of a simple harmonic oscillator, with solutions proportional to  $\exp[-(\Delta_0/\hbar\omega_c)\theta^2]$ . For typical fields  $B = 9$  T, and gap values [2]  $\Delta_0 \simeq 40$  meV, the ratio  $\gamma \equiv 2\Delta_0/\hbar\omega_c \sim 80$ . This means that the significant weight of these states is strongly localized around the node regions. Extending the limits of integration to infinity in the normalization condition (4), we obtain for the eigenfunctions

$$\Psi_{-,n}(\theta) = c_n H_n[\gamma^{1/2}\theta] e^{-(\gamma/2)\theta^2}, \quad (9)$$

where  $H_n(x)$  are the Hermite polynomials, and the coefficient  $c_n$  is

$$c_n = \sqrt{\frac{(\gamma/\pi)^{1/2}}{2^n n! [(n+2) + (5\gamma/4n) + (2\gamma)^{1/2}]}}, \quad (10)$$

$n > 0.$

The angular amplitudes obeying the periodic boundary conditions can be constructed from the above solution, Eq. (9), by inserting them into Eqs. (6) and (7) with the

As will soon become evident [cf. Eq. (11)],  $E_n \gg \bar{\mu}$ , and therefore  $\bar{\mu}$  will be neglected in the following calculations. Using the observation of Bar-Sagi and Kuper [21], and Kosztin and co-workers [22] for the Andreev Hamiltonian, the *square* of the Hamilton operator acting on  $(u_n(\phi), v_n(\phi))$  in (3) can be diagonalized with the help of a unitary transformation. The eigenvalues and the eigenfunctions of eigenvalue problems obtained in this way,

$$[-\hbar^2\omega_c^2\partial_\phi^2 + \Delta^2(\phi) \pm \hbar\omega_c(\partial_\phi\Delta(\phi))]\Phi_{\pm,n}(\phi) = \lambda_n\Phi_{\pm,n}(\phi), \quad (5)$$

are simply related to the eigenvalues and eigenfunctions,  $E_n, (u_n(\phi), v_n(\phi))$ , of the original problem (3),

$$E_n = \pm\sqrt{\lambda_n}$$

$$u_n(\phi) = \frac{1}{2} [\Phi_{-,n}(\phi) + i\Phi_{+,n}(\phi)], \quad (6)$$

$$v_n(\phi) = \frac{1}{2i} [\Phi_{-,n}(\phi) - i\Phi_{+,n}(\phi)].$$

Furthermore, the eigenfunctions of the two branches are interrelated for  $|E_n| > 0$ ,

$$\Phi_{-,n} = \frac{1}{|E_n|} Q\Phi_{+,n}, \quad \Phi_{+,n} = \frac{1}{|E_n|} Q^\dagger\Phi_{-,n}. \quad (7)$$

Here the following notation was used:  $Q \equiv -\hbar\omega_c\partial_\phi + \Delta$ ,  $Q^\dagger \equiv \hbar\omega_c\partial_\phi + \Delta$ . In the intermediate field regime the excitations of interest lie deep in the node region  $\theta = \phi - \phi_j \ll \phi_j$ , for which the  $d$ -wave potential is linear  $\Delta(\phi) \simeq 2\Delta_0\theta$ . Thus, near the nodes, Eq. (5) takes a particularly simple form

$$\Psi_{-,n}''(\theta) + \left[ \frac{E_n^2 + 2\hbar\omega_c\Delta_0}{(\hbar\omega_c)^2} - 2\frac{\Delta_0}{\hbar\omega_c}\theta^2 \right] \Psi_{-,n}(\theta) = 0, \quad (8)$$

substitution  $\Phi_{-,n}(\phi) = \Psi[\min_j\{\phi - (2j+1)\pi/4\}]$ . The overlap of the nodal states residing in two adjacent nodes is  $\exp[-\pi^2\Delta_0/8\hbar\omega_c] \sim 3.7 \times 10^{-22}$ . Clearly, quantum oscillations arising from interference between low lying nodal states located at different nodes will be significant only near  $H_{c2}$ , where  $\hbar\omega_c \sim \Delta_0$ . The eigenvalues are  $E_n^2 = 4n\Delta_0\hbar\omega_c$ , which gives two branches of eigenvalues for the original Eqs. (3)

$$E_n = \pm 2\sqrt{n\Delta_0\hbar\omega_c}. \quad (11)$$

The spacing between these states is considerably larger than the magnetic energy  $\hbar\omega_c \ll 2\sqrt{\Delta_0\hbar\omega_c} \ll \Delta_0$ . For  $B = 9$  T,  $\delta E_n = (2\gamma)^{1/2}\hbar\omega_c \sim 13$  meV, while  $\hbar\omega_c \simeq 1$  meV.

The  $n = 0$  state is anomalous, as it does not belong to either of the sets in (7). It is a so-called “zero mode,” a feature that is expected for the supersymmetric *squared* Hamiltonian [22,23]. It is worth noting that even a strongly anisotropic  $s$ -wave order parameter could, in

principle, give a discrete quasiparticle spectrum in a magnetic field. However, the conditions of normalizability required for the existence of such a state are naturally satisfied *only* for an order parameter with true gap nodes [such that  $\Delta(\phi) \sim [\partial_\phi \Delta(\phi)]_{\phi=\phi_j}(\phi - \phi_j)$  near  $\phi \sim \phi_j$ ].

Clearly, the experimental detection of the discrete nodal spectrum and, especially, the observation of the anomalous zero mode in materials suspected of having gap nodes would be quite important. Let us now find the most favorable experimental circumstances for observing these states. The nodal quasiparticles are affected by the supercurrents surrounding the vortices, which vary over a distance set by the magnetic length  $d = \sqrt{2eB/\hbar c}$  [15] where  $B$  is the applied magnetic field, and  $\hbar c/2e$  is the superconducting flux quantum. An external field of  $B = 9$  T gives  $d \approx 150$  Å. This length also gives the lattice constant of the Abrikosov vortex lattice:  $a_\square = d$ ;  $a_\Delta = (4/3)^{1/4} d$  [24]. Since the motion occurs on the background of a varying superflow, the spectrum is shifted [17] by  $\delta E_S(r) = m\mathbf{v}_F \cdot \mathbf{v}_s(r)$  typically of order  $\delta E_S \sim \Delta_0 \xi_0/2d$ . This is *not negligible* when compared to the level spacing  $\delta E_n \sim 2\sqrt{\hbar\omega_c\Delta_0} \sim 2\Delta_0\sqrt{\ell_F\xi_0}/d$  (here  $\ell_F = 2\pi/k_F \sim 0.23$  Å is the Fermi wavelength). Indeed,

$$\frac{\delta E_n}{\delta E_S} \sim 4 \left( \frac{\ell_F}{\xi_0} \right)^{1/2} \sim 0.5. \quad (12)$$

If the trajectory includes segments close to the core  $r \sim \xi_0$ , in those regions the ratio drops to  $\delta E_n/\delta E_S \sim 0.05$ . A global spectroscopic probe, such as electromagnetic absorption [9], will detect a spatially averaged response. Clearly, this also implies an average over the shift  $\delta E_S$ , which would make the resonant transitions between the discrete quasiparticle levels difficult to observe.

The situation is quite different for a scanning tunneling microscope, with which one could select with at least  $\delta r \sim 1$  Å resolution the place where electrons are injected or removed from a superconductor. The local tunneling conductance can be given as

$$\begin{aligned} \left( \frac{dI(r)}{dV} \right) &\propto -N_B \sum_{n \geq 0} \int_{-\pi}^{\pi} \frac{d\phi}{2\pi} |T(\phi)|^2 \\ &\times \left\{ |u_n(\phi)|^2 \frac{\partial f[E_n^-(r, \phi, V)]}{\partial E_n} \right. \\ &\quad \left. + |v_n(\phi)|^2 \frac{\partial f[E_n^+(r, \phi, V)]}{\partial E_n} \right\}. \quad (13) \end{aligned}$$

Here  $N_B = (\text{sample area})/2\pi d^2$  is the degeneracy of each level,  $|T(\phi)|^2$  is the square of the tunneling matrix element which, in principle, can be angle dependent [25],  $E_n^\pm(r, \phi, V) = E_n(r, \phi) \pm eV$ , and  $f(\epsilon) = [\exp(\beta\epsilon) + 1]^{-1}$  is the Fermi distribution function. The local spectrum also depends on the angle  $\phi$  through the Doppler shift

$$E_n(r, \phi) = E_n + E_S(r) \cos(\phi - \alpha), \quad (14)$$

where  $\alpha$  is the angle between the local superfluid velocity and the  $\hat{a}$  crystal axis. For a rigid and stationary

Abrikosov lattice  $\alpha$  is fixed.  $E_S(r) = mv_F v_s(r)$  is the maximum Doppler shift at a particular place  $\mathbf{r}$ . In Eq. (13) there is no summation with respect to  $k_z$ , the momentum in the  $\hat{c}$  direction. This two-dimensional approximation is especially adequate for superconducting  $\text{Bi}_2\text{Sr}_2\text{CaCu}_2\text{O}_{8+x}$  samples [26].

The important observation here is that according to Eq. (9) the Bogoliubov amplitudes  $u_n(\phi), v_n(\phi)$  are highly peaked functions around the nodal angles. Compared to  $|u_n(\phi)|^2$  and  $|v_n(\phi)|^2$ , all other factors in (13) are weak functions of the angle  $\phi$ , and can be taken outside the integral. As a consequence the integration over the angle reduces to summation over the nodal directions of the order parameter: For a  $d$ -wave superconductor,  $\phi_j = (2j + 1)\pi/4$ ,  $j = \{0, 1, 2, 3\}$ . While the tunneling matrix element along the node directions  $|T(\phi_j)|^2$  is small [25], it is nevertheless finite, as indicated by the finite zero bias conductance in tunneling experiments [11]. In the following, it is assumed that  $|T(\phi_j)|^2$  has the same value for all four nodes. The dimensionless conductance  $g(V)$  can be defined as

$$g(V) \equiv - \sum_{j,n \geq 0} \left\{ \frac{\partial f[E_n^-(r, \phi_j, V)]}{\partial(\beta E_n)} + \frac{\partial f[E_n^+(r, \phi_j, V)]}{\partial(\beta E_n)} \right\}. \quad (15)$$

In order to reveal the essential features of the above result, let us first assume that the tip of the scanning tunneling microscope is positioned on the Wigner-Seitz cell of the vortex lattice (cf. the inset of Fig. 3). For all points on the cell boundary  $E_S(r) = 0$ . At low enough temperature the quasiparticle scattering rate [27], as well as the uncertainty in  $\delta E_S(r)$  due to vortex lattice fluctuations, is smaller than the level spacing  $\delta E_n > \hbar/\tau_{\text{qp}}, \delta E_S^{\text{lattice}}$ . Under these conditions the tunneling conductance reveals (see Fig. 2) the discrete spectrum obtained in Eq. (11). Note that the amplitude of the zero mode is twice the amplitude of the finite voltage peak, since the particle and hole tunneling

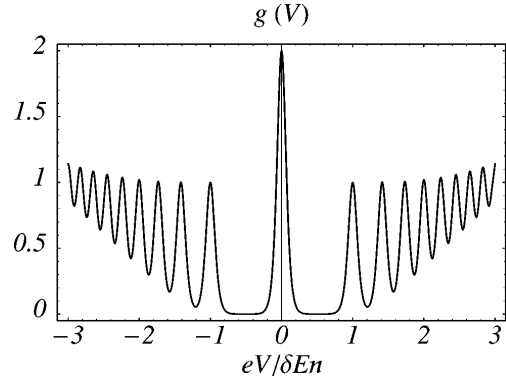


FIG. 2. The dimensionless STS tunneling spectrum  $g(V)$  on the Wigner-Seitz cell boundary, according to Eq. (15), for  $k_B T/\delta E_n = 1/24$ .

rates are the same near  $V = 0$ . This is also evident from Eq. (13).

As the tip is moved away from the cell boundary, towards one of the cores (for example, along the dashed line of the inset of Fig. 3), each peak splits up into four separate peaks, corresponding to the four nodes of the order parameter. This is illustrated in the main part of Fig. 3, where, for clarity, only the splitting of the zero bias peak is shown. The amplitudes of the split peaks are 4 times smaller than the amplitude of the single peak measured at the Wigner-Seitz cell boundary.

In conclusion, this paper addressed the problem of the quasiparticle spectrum in a  $d$ -wave superconductor in an external magnetic field. The spectrum is discrete, and the quasiparticle amplitudes are strongly peaked for momenta pointing along the node directions. An anomalous zero mode is present only if the order parameter has true nodes. As it turns out, the level spacing is smaller than the average Doppler shift due to the interaction of quasiparticles with the supercurrents circling around the vortices. Thus, in order to detect this spectrum, one needs to perform scanning tunneling spectroscopy on the Wigner-Seitz cell boundary of the Abrikosov vortex lattice, where the superfluid velocity is zero. The calculated local tunneling spectrum also indicates that slightly away from the Wigner-Seitz boundary, each peak splits into four subpeaks, as a consequence of the four different Doppler shifts arising for quasiparticles tunneling into the four nodes. The results are clearly more general than the specific case of a quasi-two-dimensional superconductor with a  $d$ -wave order parameter, and can be extended in a straightforward manner to *any layered superconductor*

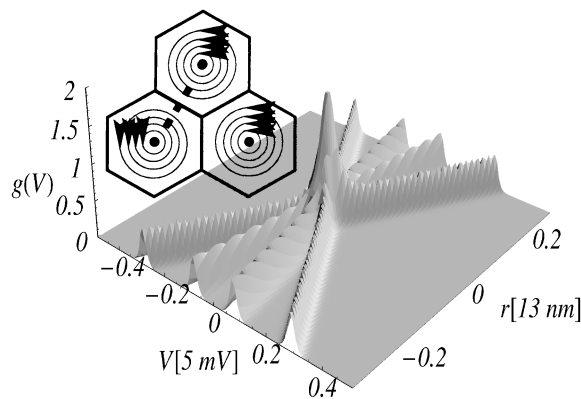


FIG. 3. Main figure: Plot of the dimensionless conductance  $g(V)$  [cf. Eq. (15)] of the *zero bias peak only*, as the position is varied along the dotted line of the inset. The parameters are  $\delta E_n = 5$  meV,  $d = 400$  Å,  $\alpha = \pi/6$ , and  $T = 6$  K. Inset: Schematic figure of a vortex lattice. The Wigner-Seitz cells, where the superfluid velocity is zero, are drawn with heavy lines; the dots correspond to the vortex cores (not on scale with the lattice constant). The suggested path for the tip of the scanning tunneling microscope is shown with a heavy dotted line.

that has gap nodes. In fact, the experiment proposed here would probe intimate details of the superconducting state, such as the *existence*, the *number*, and the *position* of gap nodes on the Fermi surface.

I thank Professor Alexei A. Abrikosov, Dr. Marcel Franz, and Dr. Ioan Kosztin for helpful discussions. This research was supported in part by the NSF under DMR91-20000 (administrated through the Science and Technology Center for Superconductivity), and the U.S. DOE, BES, under Contract No. W-31-109-ENG-38.

- [1] P. A. Lee, *Science* **277**, 5322 (1997).
- [2] J. C. Campuzano *et al.*, *Phys. Rev. B* **53**, 14 737 (1996).
- [3] See A. Pomar *et al.*, *Phys. Rev. B* **54**, 7470 (1996), and references therein.
- [4] D. A. Wollman *et al.*, *Phys. Rev. Lett.* **74**, 797 (1995); J. R. Kirtley *et al.*, *Nature (London)* **373**, 225 (1995).
- [5] C. Caroli, P. G. de Gennes, and J. Matricon, *Phys. Lett.* **9**, 307 (1964).
- [6] Y. Morita, M. Kohmoto, and K. Maki, *Phys. Rev. Lett.* **78**, 4841 (1997).
- [7] N. Hayashi *et al.*, *Phys. Rev. Lett.* **80**, 2921 (1998).
- [8] M. Franz and Z. Tesanovic, *Phys. Rev. Lett.* **80**, 4763 (1998).
- [9] K. Karraï *et al.*, *Phys. Rev. Lett.* **69**, 355 (1992); H.-T. S. Lihn *et al.*, *ibid.* **76**, 3810 (1996).
- [10] I. Maggio-Aprile *et al.*, *Phys. Rev. Lett.* **75**, 2754 (1995).
- [11] While Ch. Renner *et al.*, *Phys. Rev. Lett.* **80**, 3606 (1998), reported no bound states, they seem to be present in recent data by S. H. Pan *et al.* (unpublished).
- [12] A. Yazdani *et al.*, *Science* **275**, 1767 (1997).
- [13] G. E. Volovik, *Sov. Phys. JETP* **65**, 1193 (1987).
- [14] L. P. Gor'kov and J. R. Schrieffer, *Phys. Rev. Lett.* **80**, 3360 (1998).
- [15] P. W. Anderson, cond-mat/9812063.
- [16] K. Krishana *et al.*, *Science* **277**, 83 (1997).
- [17] M. Cyrot, *Phys. Kondens. Mater.* **3**, 374 (1965), observed experimentally by H. F. Hess, R. B. Robinson, and J. V. Waszczak, *Phys. Rev. Lett.* **64**, 2711 (1990).
- [18] G. E. Volovik, *JETP Lett.* **58**, 469 (1993); N. B. Kopnin, *Phys. Rev. B* **57**, 11 775 (1998); C. Kubert and P. J. Hirschfeld, *Phys. Rev. Lett.* **80**, 4963 (1998).
- [19] M. R. Norman *et al.*, *Phys. Rev. B* **57**, R11 093 (1998).
- [20] See, also, K. Maki, *Phys. Rev. B* **44**, 2861 (1991); M. J. Stephen, *Phys. Rev. B* **45**, 5481 (1992); P. Miller and B. L. Gyorffy, *J. Phys. Condens. Matter* **7**, 5579 (1993); M. R. Norman and A. H. MacDonald, *Phys. Rev. B* **54**, 4239 (1996); Z. Tesanovic and P. D. Sacramento, *Phys. Rev. Lett.* **80**, 1521 (1998).
- [21] J. Bar-Sagi and C. G. Kuper, *Phys. Rev. Lett.* **28**, 1556 (1972).
- [22] I. Kosztin *et al.*, *Phys. Rev. B* **58**, 9365 (1998).
- [23] E. T. Witten, *Nucl. Phys.* **B188**, 513 (1981).
- [24] A. A. Abrikosov, *Sov. Phys. JETP* **5**, 1174 (1957).
- [25] O. K. Andersen *et al.*, *Phys. Rev. B* **49**, 4145 (1994).
- [26] R. Kleiner and P. Müller, *Phys. Rev. B* **49**, 1327 (1994).
- [27] D. A. Bonn *et al.*, *Phys. Rev. B* **47**, 11 314 (1993).